Three-Dimensional Reconstruction of AR 11158 During its Emergence Phase Using SDO/HMI Observations

Georgios Chintzoglou and Jie Zhang

School of Physics, Astronomy and Computational Sciences, George Mason University, 4400 University Dr., MSN 6A2, Fairfax, VA 22030, USA

gchintzo@gmu.edu

Received ____________________; accepted ____________________

ABSTRACT

A solar active region (AR) is a three dimensional magnetic structure formed in the convection zone, whose property is fundamentally important for determining the coronal structure and solar activity when emerged. However, our knowledge on the detailed 3-D structure prior to its emergence is rather poor, largely limited by the low cadence and sensitivity of previous instruments. Here, using the 45-second high cadence observations from the Helioseismic and Magnetic Imager (*HMI*) instrument onboard the Solar Dynamics Observatory (*SDO*), we are able for the first time to determine and reconstruct the detailed three-dimensional magnetic structure of AR 11158 during the emergence phase and to characterize its magnetic connectivity and topology. This task is accomplished with the aid of the time-stacking method and advanced 3-D visualization.

We find that the AR consists of two major bipoles. The two polarities of each bipole show interesting tree-like structure, i.e. while the bottom of the polarity appears as a single trunk-like flux-tube, the top of the polarity has multiple branches, consisting of smaller and thinner flux tubes which connect to the branches of the opposite polarity that is similarly fragmented. The four roots of the two bipoles align well along a straight line, while the top branches are slightly non-coplanar. Our observations suggest that an active region, even appearing most complicated following emergence, may originate from a simple straight flux tube.

Subject headings: Sun: general — Sun: magnetic topology — Sun: surface magnetism

1. Introduction

The subject of AR emergence is one of the least understood but also a subject of crucial importance for constraining solar dynamo models and explaining what drives the solar phenomena and space weather. It is widely believed that ARs are magnetic flux-tubes that are being created over the course of the solar cycle by the dynamo process acting at a depth in the Solar Convection Zone (SCZ) (Charbonneau 2005.) Subsequently, the flux-tubes emerge through the photospheric surface giving birth to sunspots and coronal loop systems.

Observations of AR emergence indicate a high order of regularity with regard to the early stages of evolution of the bipolar AR. This regularity is implied by the Hale's and Joy's laws of magnetic polarity in sunspot groups, and the standard manner of proper motions of the small scale, mixed polarity magnetic elements that separate and coalesce into discrete polarities. Zwaan (1987) provided a toy-model explanation of AR emergence based on observations by attributing it to the subsurface structure of an AR; an Ω-shaped loop of magnetic flux with a freyed crest that brakes through the surface giving rise to the observed appearance of bipolar ARs. The work by Strous et al. (1996) and Strous & Zwaan (1999) extends this model to indclude the horizontal dynamics and the fact that many flux tubes emerge in multiple locations. Tanaka (1991) studied complex (delta configuration) ARs where they exhibit rotational proper motions during their evolution (starting as Hale's and Joy's laws incompatible towards becoming compatible) and attributed it to a knotted overall morphology. Also, Leka et al. (1996) found evidence that flux-tubes energe kink-deformed by the current they carry, thus they emerge with a 3-D structure far away from an Ω-shaped flux loop. It is difficult to determine the detailed 3-D structure of an AR, due to the limitation of previous observations in terms of spatial and temporal resolution (both ground-based and space-borne.)

There is a vast number of theoretical works which have been developed over the past four decades trying to attack the problem computationally (for a review, see Fan 2009.) However, the most popular models of emergence in the SCZ, (a) the Thin Flux Tube model (TFT, Spruit 1981) and (b) the anelastic MHD approximation, are not valid at the top layers of the SCZ (that is, 20 - 30 Mm below surface), as the flux-tubes are not thin (TFT assumption breaks down) and the velocity field is not subsonic (anelastic approximation breaks down); the reason for this invalidity lies behind the strong pressure gradient at those layers below the surface (Fan 2009; Stein 2012.) Thus we can split the SCZ into two parts, the lower SCZ and the upper SCZ ($\approx 20\,\mathrm{Mm}$.)

With the advent of computational power and sophisticated algorithms, it has been possible for "realistic" numerical experiments (i.e. fully compressible, radiative-convective 3D MHD simulations) to explore the formation of pores and sunspots (e.g. Cheung et al. 2010; also see review by Stein 2012), although the spatial domain achieved so far is still very small (the "deepest" simulations go down to a depth of 20 Mm in spite of resolving the full size of the SCZ, $\approx 220\,\mathrm{Mm}$.) Also, Radiative-convective MHD models provide no explanation on some characteristics of emerging ARs − such as the Joy's law of AR tilts and asymmetric foot-point separation − which are reproducible by global-scale models, like the TFT approximation (Caligari et al. 1995) and anelastic MHD simulations (Fan 2008.) To this date, because of the computational restrictions of our current era and the natural complexity of this task, there's no global, fully compressible MHD model yet capable in probing the evolution of flux emergence throughout the entire SCZ to the surface (Fan 2009.)

***As our current best tool in hands, anelastic 3D MHD simulations are being used where they can take well into consideration the twist of the flux-tubes, a property which is observed at the photosphere as sunspot rotation in emerging ARs (a fact that the TFT model is, by definition, incapable to simulate). From these simulations, it has been found that there's a critical factor regarding the initial twist of the flux-tubes (Linton, Fan, ?), that is, an adequate amount of twist makes flux-tubes able to rise cohesively through the SCZ and survive to reach the photosphere. However, these simulations give an order of magnitude larger twist (Murray et al. 2006) than that observed (Pevtsov et al. 2001.)

There's another question of whether a twisted flux-tube's axis rises through the photosphere, or equivalently, if flux-tube emergence happens in a bodily manner, but it still remains an open topic of theoretical debate (Abbett et al. 2000; Archontis & Török 2008; Fan 2009.) Helioseismology is currently unable to address all the aforementioned questions, not only because the spatiotemporal resolution is rather poor, but also for being extremely dependent in the sensitivity of the instruments and the stochastic nature of wave excitation (see review by Gizon & Birch 2005.)

In this letter, we present the implementation of the time stacking technique as a mean to reconstruct and study the 3-D structure of an emerging AR in great detail. The NOAA AR group 11158 presented in Figure 1, is known as the one that produced the very first X-class flare (X2.2) of the Solar Cycle 24 and its energetics have been studied thoroughly by Sun et al. (2012) . The white-light photospheric and B LOS images show a complex AR. However, with our reconstruction method, it is rather evident that AR 11158 is a much simpler origin, i.e. two colliding magnetic flux-tubes.

2. Methodology

For our task, we used high time-cadence and high spatial resolution observations (0.5 arc-sec/pixel) taken by the HMI instrument on board the SDO spacecraft (Schou et al. 2012 .) The HMI instrument is able to take full-disk maps of the LOS magnetic field every 45 seconds. [[mentioning later when the computational consideration is taken into account] we only needed to select one frame out of every ten frames from our time series dataset, reducing the effective time-cadence down to 7.5 minutes.] The starting time, t_0, of the observation was on 10-Feb-2011, 00:00:28 UT where the AR 11158 first emerges at heliographic coordinates E53S20 and the ending time of the observation was on 16-Feb-2011, 11:18:27 UT where the AR had well passed the central meridian and it was fully developed. For each of the frames, we performed a geometrical correction to get the true radial field from the LOS magnetograms and we selected a cutout of $240'' \times 200''$ with a guiding center following the AR at the Carrington rotation rate. Lastly, we moved each cutout's center from their original position on the disk towards the center of the solar disk (or better, we rotated the solar sphere for the center of the cutouts to match the solar disk center), practically eliminating the strong projection spatial effects due to each frame's different position on the spherical geometry of the solar surface. That way, we produced a uniform dataset ready to be used in our method.

Since each of the frames is a map of the B-field at the (thin) photospheric layer, we treat the subject of AR emergence in the unique following way. We proceed on making a stack using the 7.5 minute cadence 2-D cutouts [reducing the computational cost by averaging 10 images], and by starting with t_0 at the top of the stack, in principle, we reconstruct the emerging magnetic structure of the field as it is directly below the photospheric surface. As a first-order approximation, the velocity of the emergent structure is considered constant, thus each frame contributes equally to the height of the structure. For the purpose of reconstruction, we used only ≈ 4.4 days worth of data (ending on 14-Feb-2011 04:25:17 UT) instead of the full dataset, as we are mostly interested to reconstruct the early and major phase of emergence. The (x, y, z) final dimensions of the datacube are 480 pix $\times$ 400 pix $\times$ 800 pix.

3. Results

In Figure 2 we present the resulted three-dimensional reconstruction by showing the iso-surfaces in the 3-D data-cubes for two representative, constant values of the normal to the surface component of the magnetic field; one, at 1100 G, which shows the "skeleton" of the structure, i.e. the core structures of each sunspot/magnetic element of the AR, and another one, at 400 G, which shows finer structures that envelope the "skeleton" structure of 1100 G. In the bottom frame (1100 G) of Fig. 2, we show, in color, which 3-D magnetic structure (P1, N1, P2, N2) corresponds to those we show in Figure 1. The color scheme we adopt is to aid our intuition for studying a magnetic flux-tube system, i.e. blue (positive) is the ascending part of the magnetic tube and red is the descending part (negative), pointing into the sun. However, we will be using the terms "bipole" or "flux-tube" interchangeably, whenever referring to a certain group of P1N1 or P2N2.

In the 1100 G, instead of coherent flux-tubes, we get a very fragmented, branch-like appearance in both bipoles, as a result of the continuous emergence of small magnetic features. Note that the small magnetic features have a remarkably ordered, "swarm"-like collective behavior, separating in terms of polarity and coalescing in "tree-trunks" − i.e. the individual polarities of the quadrupolar AR − signifying a deeper relation of all the small magnetic features with a large-scale emerging structure. The positive polarity P1, which now consists of several "branches", connects to its corresponding negative system of branches (N1), and P2 connects to N2. In other words, each of the pairs P1N1, P2N2, forms two neighboring, flux-tube systems. It is easy to note that the (fragmented) tube segments P1 and N1, and P2 and N2 are not closing at their apex, since at this location, the field is weak and mostly transverse to the LOS. However, if we go down to lower B-field iso-surfaces, i.e. 400 G, we can clearly see an almost closed system of adjacent, small branch-like arches, that (almost) continuously emerge through the gap between the space left out from each individual bipole's foot-point separation.

***See online material for a video fly-by around the two iso-surfaces [It is excellent to make these animations].

3.1. Indication for bifurcation in longitude and latitude

At a first sight, AR 11158's magnetic topology seems rather complex; however, the tendency for collinearity and coalescence of the like polarities of the bipoles at the bottom of the 3-D cube, suggests that both flux-tubes might be related, even originating from the same parental magnetic flux-tube. This picture is therefore suggesting that a sub-photospheric flux-tube has been bifurcated both in longitude and latitude. Also, for each bipole, the asymmetric polarity separation suggests flux-tubes with an oblique lambda-shape (with the leading leg being more tilted than the following) instead of axisymmetric omega-loops. This can be understood in terms of the Coriolis force acting on a rising flux-tube, as discussed by Caligari et al. (1995) with the TFT approximation and also reproduced using anelastic MHD models (Abbett et al. 2001.)

3.2. Indication for bifurcation in height

Although the 3-D visualization presented herein suggests there are certain evolutionary similarities in both bipoles, those can be regarded as qualitative similarities only. For instance, apart from the aforementioned properties we characterized, a careful look on the data-cubes reveals a kind of a mutual symmetry for both bipoles, i.e. for each bipole, there seems to be a two-phase evolution − or, equivalently, a "grouping" of the individual small branches to just two −but larger− groups we dub "Mega-Branches" ("Mega-Branch-α" and "Mega-Branch-β" or for short "MBα" and "MBβ", with "MBα" preceding "MBβ" in time, as illustrated in Figure 2.) Nevertheless, a more thorough study of the magnetic morphology of the AR 11158 should include the time-flux profile to characterize the temporal evolution in a more quantitative manner.

In Figure 4 we calculate the magnetic flux time-profile for each individual polarity of the AR, i.e. P1, N1, P2 and N2, and we overplot each polarity's unsigned profile in the same graph. According to this plot, P1N1 (solid lines) is the first one that emerges and it is followed by the second bipole, P2N2, about six hours later (dashed lines). From the Flux time-profile in Fig. 4 we see that for an individual bipole (i.e. N1P1 and N2P2) the magnetic flux of its positive and negative polarity is − to a first order − similar. Also, for both bipoles, two major flux-injection phases are identified, with the initial one being moderate ("MBα") and the later one ("MBβ") being a very much stronger "flux-surge." Those phases are understood as the two adjacent, flux "fronts" or flux-tube "Mega-branches" as it is also suggested by the 3-D reconstruction of Fig. 2. In each of the bipoles, the Mega-Branch that arrives first at the photosphere, "MBα", appears somewhat weaker and fragmented whereas the branch that arrives $\approx$2 days later, "MBβ", is much stronger. Obviously, even this secondary emergence or "surge" event consists of multiple branches; the polarity separation is much faster compared to that in "MBα", as it can be seen in Figure 2. Like we already mentioned, these flux-surge branches can be grouped as a whole into one "Mega-Branch-β" (i.e. see also onsets of N1-MBβ, N2-MBβ in Fig. 4) for each dipole, as also suggested by the Flux vs. time diagram. Thus, for each dipole we have a bifurcation in height as well (See Figs. 2, 3).

***Should I discuss the bifurcation in terms of initial twist, if present? I haven't measured the twist...

3.3. Non-planarity, tilt, and displacement of the flux-tubes due to collisions

Flux tubes are non-planar when they first emerge (i.e. top Mega-Brances) through the quiet sun (see online video). However, right before the emergence of the "flux-surge" in both of the bipoles, there is a strong pushing-aside of the already emergent Mega-Branches ("MBα's") in a manner like they seem to "know in advance" about the arrival of the stronger "flux-surge" tubes (or "MBβ's"), suggesting that the "MBβ's" interact/collide sub-photospherically with the trunks of the "MBα" tubes. At a later time, i.e. at the bottom of the data-cube, the polarities assume the "correct", Joy's law-compliant tilt. In strong flux emergence events, the observed separation of polarities and the magnetic flux build-up usually don't last more than 3 days (Fan 2009). Moreover, the Joy's law tilt of the ARs is being "locked" to a value weakly dependent on the latitude of the group, after emergence has stopped. These facts suggest that there might be a process that disconnects the flux-tubes from their roots, a process called dynamic disconnection (Fan et al. 1994.)

Also, the polarity separation brings the leading trunk of N2P2 to collide with the following trunk of N1P1. This has also an impact on how coherent the N1 polarity looks with respect to the N2. Polarity N1, which initially is fragmented, is being hold from maintaining its fragmented appearance because of P2 pushing it against each other causing it to appear more cohesive (see Fig 1 d,e,f and Fig 2.)

In the table we provide the total flux of each Mega-branch's polarity along with information on the duration of emergence and the flux-emergence rate, as deduced by the linear fits of Figure 4. Although the flux-emergence rates are different, the duration of emergence for each bipole's Mega-Branch-α is somewhat comparable, given the almost co-temporal appearance of Mega-Branch-β for both bipoles. However, bipole N1P1 relaxes quite fast as a whole but also as compared to the N2P2 which builds up more flux with time. Interestingly, while the N2-MBβ polarity flux seems to be "relaxed" as well (also being the isolated, easternmost negative polarity), P2-MBβ flux is still increasing, possibly because of the interaction of P2-MBβ with N1-MBβ at their neutral line, where reconnection has potentially occurred at the photospheric layer, after the X2.2 flare on 15-Feb-2011, 01:58 UT (Wang et al. 2012.)

4. Discussion and Conclusion

In this letter, we presented a novel technique for studying the 3-D structure of buoyant flux-tubes rising through the solar surface. It is not the first time that time-stacking has been applied to study ARs, e.g. observational inferences on the nature of delta-configuration ARs by Tanaka (1991). Leka et al. (1996) used it to demonstrate the twist in emerging ARs and found evidence that they carry electrical currents before they emerge. However, to our knowledge, this is the first implementation of the time-stacking technique to reconstruct the detailed 3-D structure of an AR, using advanced visualization and high resolution SDO/HMI data.

At least in the early stages of emergence, the emerging magnetic structures are two non-planar (both mutually and individually) neighboring bipoles, but a more detailed picture reveals a bifurcated structure for both bipoles, in longitude, latitude and height. In the low B-field iso-surfaces, multiple magnetic arches can be observed to emerge in a continuous manner, with the like-polarities coalescing and aligning with time. The 3-D reconstruction provided indications that Mega-branches could be originating from the same flux-tube below the photosphere. Last, we find that there's a dual-phase evolution for both bipoles, as suggested by both the 3-D reconstruction and the flux time-profile of the AR, providing further evidence for a bifurcation in height and flux-tubes of common origin.

This study considered that the proper motions of magnetic elements seen on the photospheric magnetograms are produced by emergence and not by surface plasma flows. It is very hard to believe the opposite happens, since from the proper velocities of the magnetic elements (100-500 $m\,sec^{-1}$), the dynamic pressure is $\approx 10^5$ smaller than the magnetic pressure we observe on the different polarities (Tanaka 1991.) Therefore, we are confident to interpret that what we can reconstruct with our method is by large, a real 3-D structure braking through the photosphere.

It is interesting to note that the crude 3-D morphology of the AR 11158 −for each bipole as well as overall− exhibits all the qualitative characteristics of the TFT approximation. The TFT model's successes in reproducing observations are well known, although it is not valid when the flux-tube is close to the surface (Caligari et al. 1995.) The same qualitative characteristics of the TFT were reproduced in incompressible MHD simulations by Abbett et al. 2001 by including the Coriolis force due to the solar rotation, in order to study its effects on the fragmentation of flux-tubes. This simulation reproduces the non-axisymmetrical morphology that arises due to the Coriolis force. From our reconstruction it is evident that we have such an assymetry. The fact that we observe it, is suggesting that the upper convection zone has not a severe impact in altering the magnetic morphology that flux-tubes have while transversing the lower convection zone, after they are born. Also, the large initial longitudinal separation of the bipoles may have happened deep in the SCZ as it is hard to imagine the non-axisymmetrical morphology that both bipoles possess, to happen at heights close to the surface, since this is readily explained by the act of Coriolis force, throughout the journey of the tubes in the SCZ. Thus, we conclude that even the bifurcations have happened at an early stage in each tube's evolution. However, the small arch-like magnetic "fibers" may be because of the large pressure gradient in the upper convection zone.

We will discuss the true magnetic vector 3-D structure by using vector observations from the SDO/HMI instrument, in a subsequent publication.

G. Chintzoglou wishes to thank Dr. M. Linton and Dr. Y. Fan for valuable discussions, and Prof. C.E. Alissandrakis for inspiring conversation and encouragement.

REFERENCES

Abbett, W. P., Fisher, G. H., & Fan, Y. 2000, ApJ, 542, 1119

—. 2001, ApJ, 546, 1194

Archontis, V., & Török, T. 2008, A&A, 492, L35

Caligari, P., Moreno-Insertis, F., & Schussler, M. 1995, ApJ, 441, 886

Charbonneau, P. 2005, Living Reviews in Solar Physics, 2, 2

Cheung, M. C. M., Rempel, M., Title, A. M., & Schüssler, M. 2010, ApJ, 720, 233

Fan, Y. 2008, ApJ, 676, 680

—. 2009, Living Reviews in Solar Physics, 6, 4

Fan, Y., Fisher, G. H., & McClymont, A. N. 1994, ApJ, 436, 907

Gizon, L., & Birch, A. C. 2005, Living Reviews in Solar Physics, 2, 6

Leka, K. D., Canfield, R. C., McClymont, A. N., & van Driel-Gesztelyi, L. 1996, ApJ, 462, 547

Murray, M. J., Hood, A. W., Moreno-Insertis, F., Galsgaard, K., & Archontis, V. 2006, A&A, 460, 909

Pevtsov, A. A., Canfield, R. C., & Latushko, S. M. 2001, ApJ, 549, L261

Schou, J., Scherrer, P. H., Bush, R. I., et al. 2012, Sol. Phys., 275, 229

Spruit, H. C. 1981, A&A, 98, 155

Stein, R. F. 2012, Living Reviews in Solar Physics, 9, 4

Strous, L. H., Scharmer, G., Tarbell, T. D., Title, A. M., & Zwaan, C. 1996, A&A, 306, 947

Strous, L. H., & Zwaan, C. 1999, ApJ, 527, 435

Sun, X., Hoeksema, J. T., Liu, Y., et al. 2012, ApJ, 748, 77

Tanaka, K. 1991, Sol. Phys., 136, 133

Wang, S., Liu, C., Liu, R., et al. 2012, ApJ, 745, L17

Zwaan, C. 1987, ARA&A, 25, 83

This manuscript was prepared with the AAS LaTeX macros v5.2.

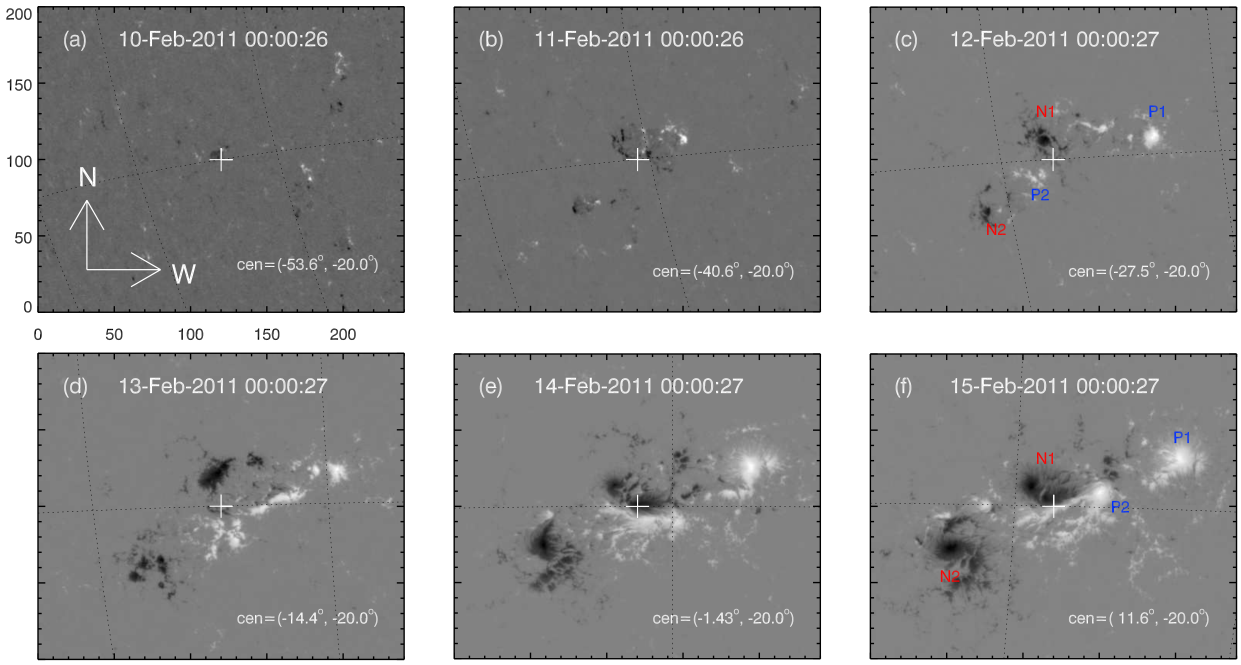

Fig. 1.— The first 6 days of evolution of the AR 11158 as observed with the SDO/HMI LOS magnetograph. The individual polarities are named after which bipole emerged first, e.g. bipole 1, where we name its negative polarity N1 and its positive P1, and with N2 and P2 emerging at a later time. The white cross shows the position of the guiding center of the $240'' \times 200''$ FOV at a fixed heliographic latitude $\phi = -20°$.

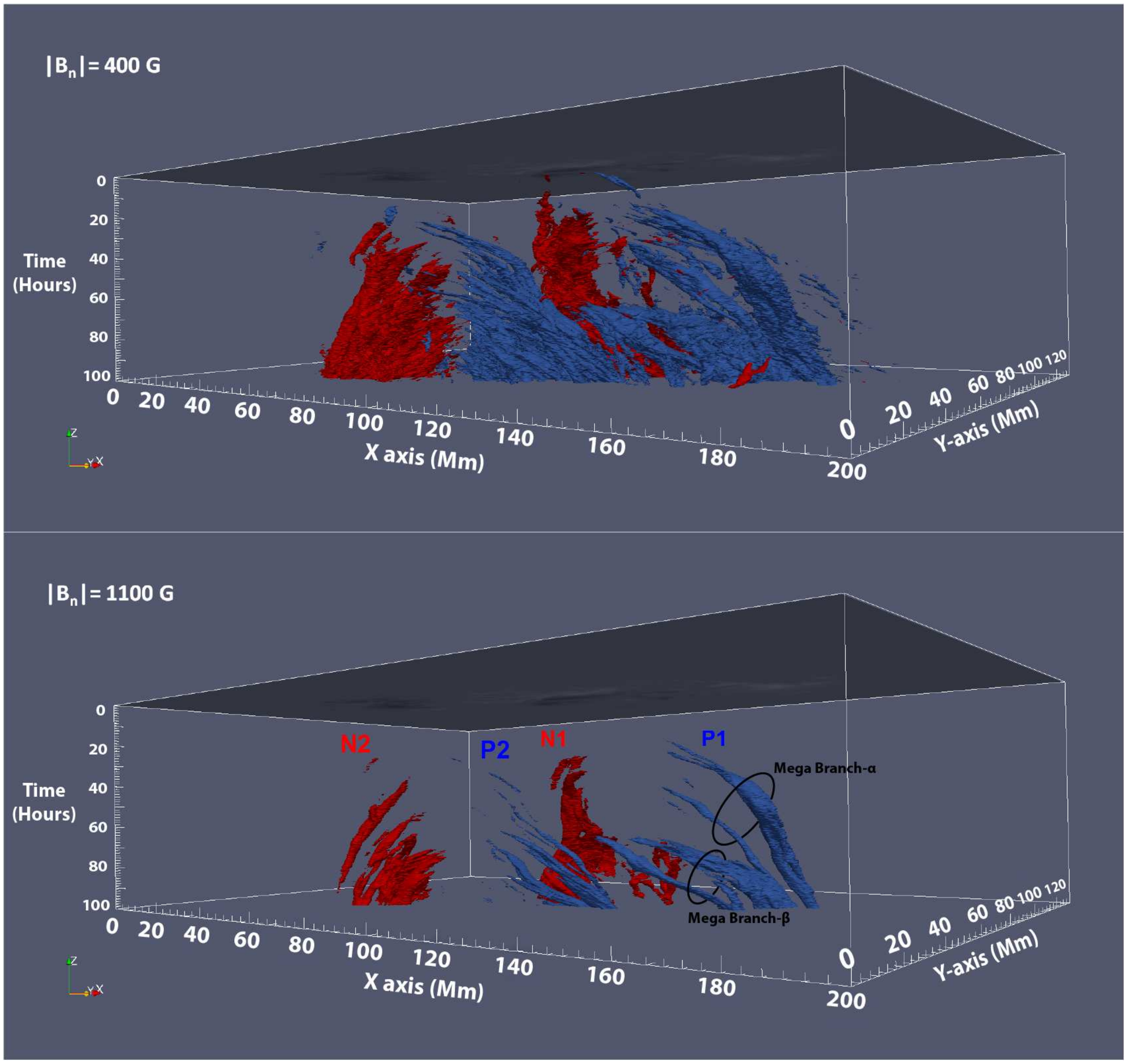

Fig. 2.— The 3-D reconstruction of AR 11158 using the time-stacking method on SDO/HMI LOS magnetograms. The flux-tubes shown here are at $|B_n| = 400$ G (up) and 1100 G (down). The color scheme adopted for visualizing the magnetic polarities is "Doppler shift"-like, i.e. red (negative B) is pointing inward to the sun and away from the observer and blue (positive B) is outward, i.e. pointing towards the observer. On top of each datacube is the last HMI LOS frame of the cube, i.e. the bottom frame, on 14-Feb-2011 04:25:57. The presented duration of the observation is 100.4 hours. The positive X-axis direction is westward and Y-axis northward. The length of the X-axis is roughly comparable with the height of the Solar Convection Zone (SCZ), i.e. about 200 Mm.

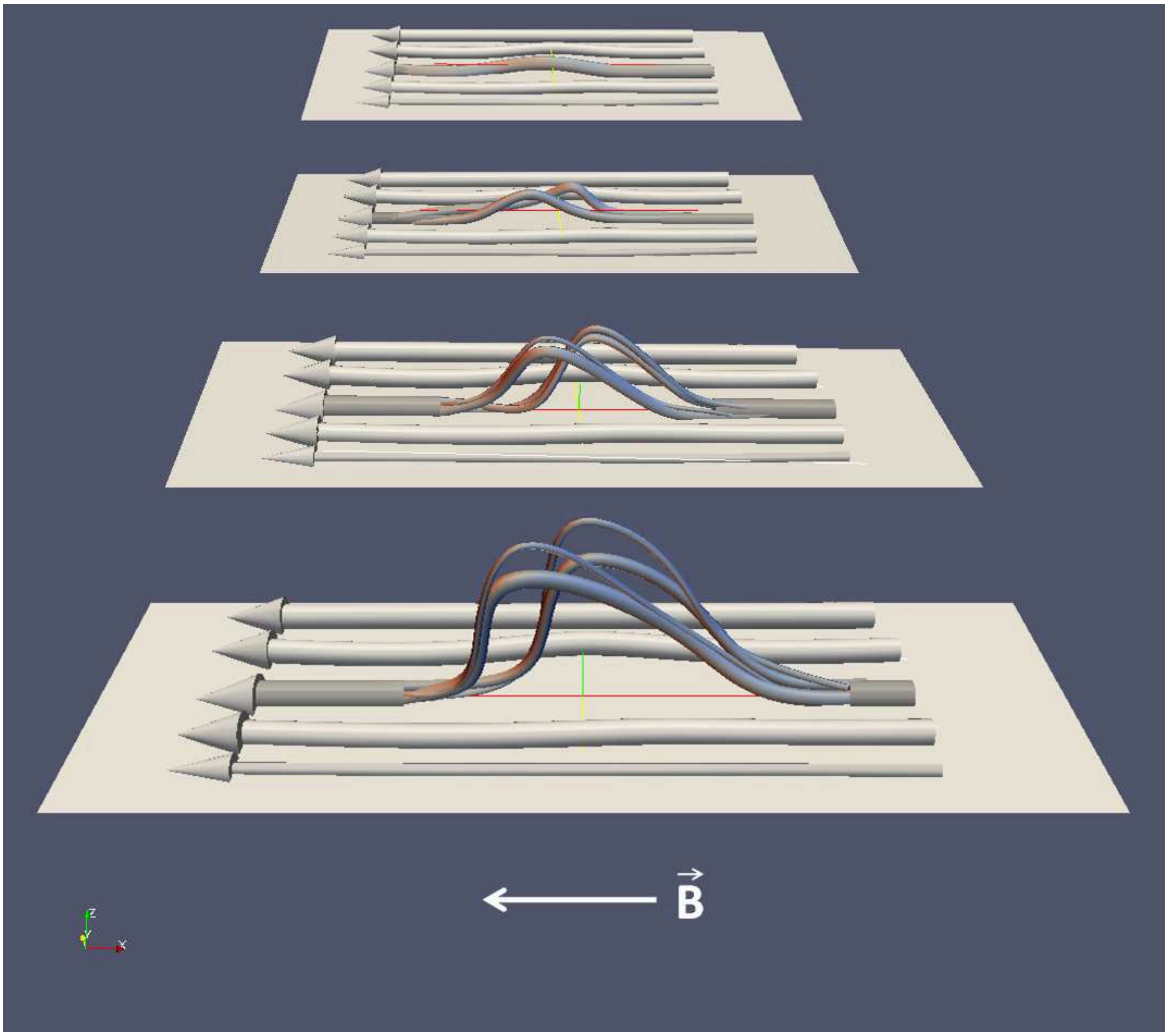

Fig. 3.— Model sketch of the emergence phase of a twin flux tube AR under the photosphere. The plane is the depth in the SCZ that B-fields originally reside. The cylindrical structures shown at that plane in the SCZ are the flux-tubes of the toroidal field, generated by the solar dynamo process. For flux tubes created in the South hemisphere during Solar Cycle 24 (like those of the AR 11158), the magnetic field vector along the tubes is directed from West-to-East (here from right-to-left), as dictated by Hale's law of polarity and the Babcock-Leighton dynamo theory. The flux-tubes develop an asymmetry due to the Coriolis force (Caligari et al. 1995.)

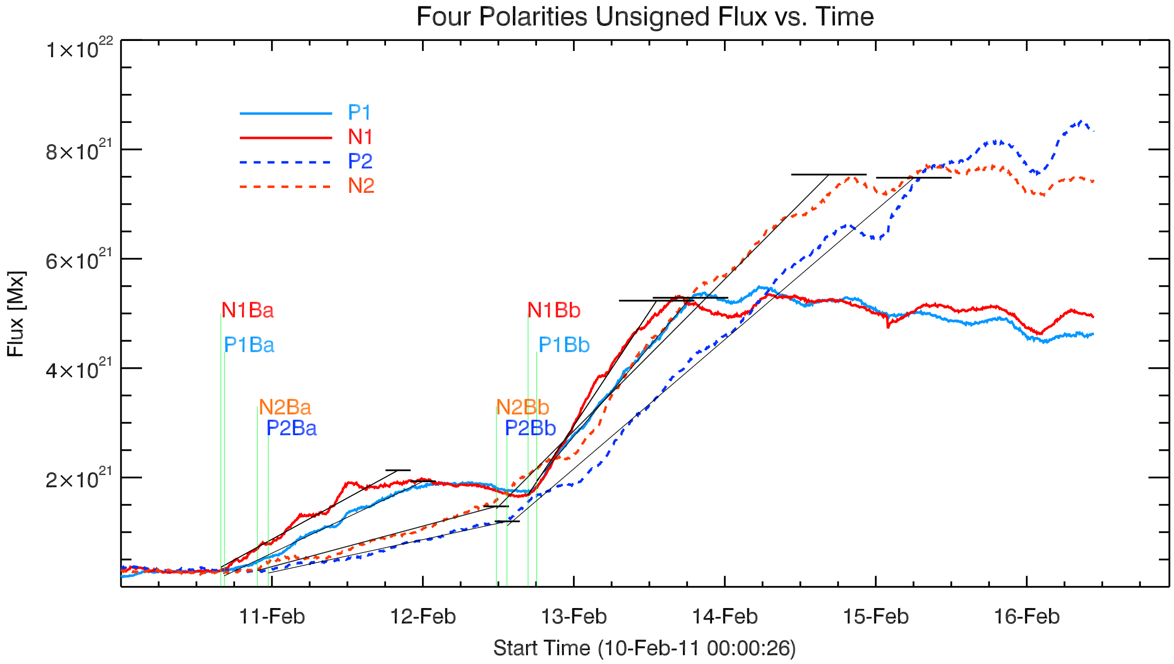

Fig. 4.— The time evolution of the flux for the bipoles N1P1 (solid lines) and N2P2 (dashed) suggests that both have an early emergence phase (i.e. "MBα") or "front" of flux, followed by a strong flux "surge" (or "MBβ") as also can be seen in Fig 3. Note the persistent lagging of the positive, i.e. leading polarities, P1 and P2 with respect to the following N1 and N2. See Table with information on the onset/end of emergence, flux injection rates and total flux for each of the branch polarities. The green lines denote the onset of emergence events. Black line fits are ending with an error bar in time, showing the reading error on the end time of emergence (± 2 h for MBα's, ± 6 h for MBβ's) We used the negative polarities to define when emergence stops as they are perpendicular and show less complexity in the flux time-profile.

Table 1. New-Emergence Rate, Total Flux emerged and duration of emergence for each polarity of the Mega-Branches as measured from Fig. 4

Bipole	Polarity	Mega-Branch	Rate[a]	Total[b]	Start Time	End Time	Duration[c]
1	P1	MBα	1.52	2.71	10-Feb 16:27	12-Feb 00:00	31.66
		MBβ	3.79	7.12	12-Feb 18:06	13-Feb 18:30	24.50
	N1	MBα	1.75	2.82	10-Feb 15:52	11-Feb 20:03	28.16
		MBβ	4.82	5.69	12-Feb 16:31	13-Feb 13:10	20.50
2	P2	MBα	0.69	2.18	10-Feb 23:24	12-Feb 13:21	37.99
		MBβ	2.73	22.27	12-Feb 13:21	15-Feb 06:00	64.64
	N2	MBα	0.91	2.58	10-Feb 21:40	12-Feb 11:40	39.99
		MBβ	3.37	16.57	12-Feb 11:40	14-Feb 09:10	43.51

[a]New-Flux Emergence Rate in 10^{16} $\mathrm{Mx\,s^{-1}}$

[b]Total Flux Emerged ($\times 10^{23}$ Mx) in the corresponding time duration

[c]Duration in hours